ELSEVIER

Journal of Molecular Catalysis A: Chemical 119 (1997) 165–176

JOURNAL OF MOLECULAR CATALYSIS A: CHEMICAL

Energetics and diffusion of butene isomers in channel zeolites from molecular dynamics simulations

F. Jousse *, L. Leherte, D.P. Vercauteren

Institute for Studies in Surface Science, Laboratoire de Physico-Chimie Informatique, Facultés Universitaires Notre-Dame de la Paix à Namur, B-5000 Namur Belgium

Received 4 June 1996; accepted 12 September 1996

Abstract

We have investigated the minimum energy positions and the short time self-diffusion of butene isomers in 6 zeolite structures: TON, MTT, MEL, MFI, FER, and HEU. The minimum energy positions, and the corresponding interaction energies, reflect essentially the steric interaction between the guest molecule and the host zeolite walls. It is shown that in all structures except zeolite TON, *trans*-2-butene diffuses faster than the other isomers, while in all cases except for TON and MTT, the diffusion of isobutene could not be followed during a 200 ps molecular dynamics run. In zeolite TON the ratio of isobutene versus linear butene self-diffusion is larger than in the other zeolites, which indicates that in this particular structure, diffusion is probably not the rate-limiting process to butene isomerization.

Keywords: Butene; Zeolites; Diffusion

1. Introduction

The skeletal isomerization of butene has gained considerable interest in the past years, due to the potential use of isobutene as a precursor to MTBE, a high octane gasoline additive. Acid zeolites have been shown to constitute very efficient catalysts for this reaction [1], which initiated numerous experimental studies aiming at pointing out the best catalysts, and the reasons for their efficiency [2–14]. Among the acid zeolites, it was found that ferrierite, a zeolite whose framework presents two interconnected perpendicular channels, one composed of 10 tetrahedral atoms (10-T) and the other of 8 tetrahedral atoms (8-T), shows a very good selectivity toward isobutene [8,12]. The efficiency of this zeolite seems not to be related to its channel system, as shown by the increase of catalytic activity after coking and therefore blocking of the channels [12,13]. However, in other zeolites like the protonated form of clinoptilolite [14], there seems to be a direct link between the channel system and the selectivity toward isobutene. Hence, there is an interest to study further the diffusion of the various butene isomers in similar interesting channel type zeolites, in order to find clues regarding how the selectivity toward isobutene could be improved. Particularly, in this paper we present results of molecular mechanics and dynamics simulations of the adsorption and diffusion of the 4 butene

* Corresponding author.

PII S1381-1169(96)00480-3

isomers in 6 zeolite models presenting different types of channels, in order to determine the influence of their shape, size, and type of connections on the diffusivities of the guest molecules.

We chose to work with 6 zeolite types [15] in which skeletal isomerization of butene has been studied experimentally: the two zeolite families MTT (ZSM-23) and TON (THETA1 or ZSM-22), which present unidirectional straight 10-T channels, with a channel size of 4.5×5.2 Å and 4.4×5.5 Å, respectively; zeolite MEL (ZSM-11), whose 3-dimensional structure is built from two identical straight 10-T channels of 5.3×5.4 Å perpendicular to each other; the 3-dimensional framework of zeolite MFI (ZSM-5) composed by a straight 5.3×5.6 Å 10-T channel and a zigzag 5.1×5.5 Å 10-T channel system; zeolite FER (ferrierite or ZSM-35), which presents a 10-T straight channel (4.2×5.4 Å) interconnected with a perpendicular straight 8-T channel (3.5×4.8 Å); and finally, zeolite HEU (heulandite), with elliptical 10-T channels (3.0×7.6 Å) and 8-T channels (3.3×4.6 Å) along [001], connected to 8-T channels (2.6×4.7 Å) along [100].

All these zeolite structures present numerous different isotopic frameworks [15] and therefore many different possible Si/Al ratios. As we are interested here mainly in the influence of the size, shape, and connectivity of the channels on butene self-diffusion, regardless of its chemical composition, we chose to work with the all-silica end member for each zeolite family. However, in order to add to the relevance of this computational study, a comparison will be made between the results obtained for H-ferrierite with a Si/Al 8 [16] and all-silica ferrierite.

After a short description of the procedure used for the computational simulations in Section 2, we present in Section 3 the minimum energy positions, the corresponding energies, and the computed self-diffusivities of the various butene isomers in each zeolite family, as well as a relevant discussion on how these quantities may be related to the shape and size of the guest molecules as compared to the host zeolite channels.

2. Computer experiments

All results were computed using the cff91-czeo forcefield, available within the Discover software [17] of Biosym Technologies. This forcefield was primarily chosen because it integrates terms explicitly derived to treat the hydroxyl group in zeolites [18]. Its main features are that of a generalized valence forcefield, representing bonded interactions by 2, 3, and 4-body terms and non-bonded interactions by a 6–9 van der Waals potential and Coulombic interactions. The zeolite structures were optimized using this forcefield, and the results may be used as a test of its capabilities to predict aluminosilicate structures; no symmetry constraints were applied during the optimization.

The minimum energy positions of the butene isomers within the zeolite channels were identified using the Monte-Carlo docking procedure of Freeman et al. [19]: one hundred initial configuration of the guest molecule–host zeolite complex were randomly chosen and optimized, including coulombic interactions. The zeolite structures were allowed to relax with the sorbed molecule. Identifying the minimum energy positions allow to determine the relevant interactions acting on the guest molecule, and the origin of their influence.

The self-diffusivities of the butene molecules were then investigated by Newtonian molecular dynamics. The simulation cell consisted of the required number of the optimized unit-cells to build an approximately $20 \times 20 \times 20$ Å box, in which 4 butene molecules were allowed to move under periodic boundary conditions. The zeolite frameworks were held fixed during the molecular dynamics simulation. The same forcefield as for the docking study was used, that is, cff91-czeo, but without coulombic interactions; we have shown indeed that they have almost no

influence on the diffusivities, even in H-FER [16].

After a 50 ps equilibration run in the NVT ensemble to achieve equilibrium at the desired temperature of 623 K corresponding to the experimental conditions used for butene isomerization in H-FER [8], a 200 ps simulation run with a 1 fs time-step in the NVE ensemble was performed and used to collect the data. From these data the mean-square displacement (MSD) and the velocity autocorrelation function (VACF) of the center of mass of the butene isomers were computed. These allow to evaluate the self-diffusion coefficient by two methods, that is, from the slope of the MSD versus time by the Einstein relation and from the integration of the VACF [20]. The Fourier transform of the VACF were also computed, in order to give information on the low frequency motions of butene isomers in these zeolites. All calculations were performed on IBM RS/6000 model 340 and 560 computers with 128 Mb memory.

Table 1
Cell dimensions determined from the optimization of the structure with the cff91-czeo forcefield of Biosym. No symmetry constraints were used during optimization

Zeolite code		*a*	*b*	*c*	
TON	expt.	13.86	17.42	5.04	Ref. [21]; no Al
	expt.	13.84	17.42	5.04	Ref. [22]; no Al
	calc.	14.13	17.92	5.25	
MTT	expt.	5.01	21.52	11.13	Ref. [23]; Si/Al = 166
	calc.	5.25	22.16	11.44	
MEL	expt.	20.07	20.07	13.41	Ref. [24]; no Al
	expt.	20.06	20.06	13.40	Ref. [25]; no Al
	calc.	20.46	20.46	13.72	
MFI	expt.	20.02	19.90	13.38	Ref. [26]; Si/Al = 300
	expt.	20.07	19.92	13.42	Ref. [27]; Si/Al = 86
	calc.	20.48	20.40	13.70	
FER	expt.	18.72	14.07	7.42	Ref. [28]
	expt.	18.81	14.09	7.43	Ref. [29]; giant crystals
	calc.	19.07	14.31	7.55	
H-FER	expt.	19.16	14.13	7.49	Ref. [30]; Si/Al = 5.5
	expt.	19.23	14.15	7.50	Ref. [31]; Si/Al = 4.3
	expt.	19.22	14.12	7.49	Ref. [32]; Si/Al = 4.1
	calc.	19.28	14.40	7.59	Si/Al = 8
HEU	expt.	17.77	17.95	7.44	β = 116.46; Ref. [33]
	calc.	17.88	17.79	7.50	β = 116.56

3. Results and discussion

3.1. Structure

Table 1 reports the dimensions of the unit-cell determined by an unconstrained optimization of the zeolite structure with the cff91-czeo forcefield. All the calculated cell parameters refer to the all-silica structure, except for H-ferrierite where we have included a structure with Si/Al = 8. In the latter case, 4 silicon were substituted by alumina on a T2 tetrahedron, and protons were linked to the neighbor oxygen in position O7 of the 8-T ring; see Ref. [16] and Fig. 2 of the present paper for details on the position of the protons.

The optimization of the structure leads to cell parameters in general good agreement with the experimental ones, as the largest error is less than 3%. However, we note a slight overestimation of the distances, which was also observed on the original test set of the potential [18]. This probably originates from a short overestimation of the Si–O bond distances. The increase of the cell dimensions in going from FER to H-FER is in agreement with the experimental observation.

4. Minimum energy positions

For each host–guest system, several stable minimum energy positions may be found; however, in all cases only one or two energetically and topologically different classes of minimum energy positions exist. Table 2 lists the minimum interaction energies in the main classes of energy sites found by the docking procedure. The interaction energy to which we refer here is the energy of the host–guest system minus the energy of each component evaluated separately. The main classes of minimum energy positions correspond in most cases to molecules sorbed in different channels; the dimensions of the chan-

nels used in the calculation are therefore also listed in Table 2. There is considerable uncertainty in the radius of the oxygen ions to use to evaluate the channel dimensions [34]; we used here a diameter of 3 Å, which, in connection with the different size of the unit-cell, leads to values that may be different from those listed in the atlas of zeolite structures [15] and given in Section 1.

The results obtained on FER and H-FER allow to determine the influence of the protons in these calculations. In both cases, two stable minimum energy positions were found, at the intersection between the 8-T and 10-T channels, and in the cavities located along the 10-T channels. The orientation of the molecules in these sites is the same. However, the corresponding energies are quite different, as they are more than 10 kJ/mol lower for H-FER than for FER. The contribution from the coulombic energy in all cases remains small (from 0.1 to 1.6 kJ/mol for FER, from 0.4 to 3.5 kJ/mol for H-FER), and cannot account for the differences, which essentially arise from steric effects, due to the Al substitution and the interaction with the protons. In the case of FER, the sites in the 8-T cavities are the most stable ones (except for *trans*-2-butene), while they are destabilized by 2 to 7 kJ/mol for H-FER, thus showing that the steric effects of the protons is more pronounced in these smaller 8-T cavities. This comparison shows again the small influence of the electrostatic effects in this description and with this potential; it corroborates the preceding study [16], in which we have shown that coulombic interactions have little or no influence on the butene self-diffusion in ferrierite. However, one may wonder if the influence of the protons is accurately taken into account by these steric effects only. Beside the actual chemical link between the zeolitic proton and the sorbed molecule, which has been extensively studied theoretically and experimentally (for some recent reviews and results see, e.g. Ref. [35]) and cannot be reproduced with our classical forcefield, there is likely to be some electrostatic interactions via the molecular multipole moments and polarizability; these interactions have been shown to be important in the case of even non-polar molecules in cationic A zeolites [36]. Indeed, a recent ab initio study of the interaction of unsaturated carbons with a $H_3Si(OH)AlH_3$ cluster modeling a zeolitic Brønsted site has shown that the interaction is predominantly electrostatic [37]; with ethylene, it amounts to −13.6 kJ/mol. Following the

Table 2
Minimum interaction energies (kJ/mol) of butene isomers in the silica form of zeolites TON, MTT, MEL, MFI, FER, and HEU, and in H-FER (Si/Al = 8), computed with the cff91-czeo forcefield of Biosym

Zeolite code		Channel Å × Å	1-butene	*Cis*-2-butene	*Trans*-2-butene	Isobutene
TON	[001]	4.7 × 5.4	−47.1	−44.7	−49.0	−38.6
MTT	[100]	4.3 × 4.6	−49.2	−46.2	−46.7	−47.0
MEL	[100]	5.4 × 5.6	−44.1	−43.6	−42.7	−39.8
	[010]	identical				
MFI	[010]	5.4 × 5.5	−44.7	−43.4	−43.6	−39.3
	[100]	5.2 × 5.3	−44.4	−44.3	−43.7	−41.0
FER	[001] [a]	3.8 × 5.4	−46.0	−46.3	−46.7	−44.6
	[010]	3.1 × 4.6	−49.7	−49.0	−46.1	−49.3
H-FER	[001] [a]	4.1 × 5.6	−38.6	−35.7	−38.0	−33.7
	[010]	3.2 × 4.6	−31.5	−33.9	−30.3	−27.4
HEU	[001] [b]	3.0 × 7.3	−47.3	−45.9	−45.6	−43.9
	[001] [b]	3.3 × 4.6	−45.3	−45.3	−46.9	−42.6
	[100]	2.4 × 4.5				

[a] Energy at the intersection between the 10-T channel along [001] and the 8-T channel along [010].
[b] Energy at the intersection between the channels along [001] and the 8-T channel along [100].

advice of the referee, we may add this value to the minimum energies computed for the interaction of butene in H-FER; the resulting values are very close to the ones computed in FER, which suggest that the destabilizing steric effects of the protons are compensated by the electrostatic interactions.

Once we have shown that the interaction is mainly (if not only) steric, the positions and minimum energies in the different channel zeolites listed above is easily understood in terms of confinement effects and shape complementarity between the guest molecule and the zeolite wall.

In the single channel zeolites TON and MTT, the guest molecules are located along the channel axis, near the center of the channel; confinement effect is most visible if we compare the minimum energy positions in MEL and MFI to those found in FER and HEU: in the first zeolites, with larger channels, the molecules are located in the channels but out of the intersections between the channels, while in the smaller channel zeolites FER and HEU the molecules are located at the intersection between the channels. This is exemplified by Figs. 1–4, which show the minimum energy sites (MES) for isobutene in FER, H-FER, MFI, and MEL, respectively. The MES in FER and H-FER are very similar; note the distortion of the network of H-FER due to the Al and protons. As discussed earlier, the protons seem not to attract isobutene, which is probably an artefact of the forcefield used. The destabilization of the minimum interaction energy is clearly due to the steric influence of the protons, and is larger in the smaller cavities along the 8-T channels than in the 10-T channels: the sum of the inverse

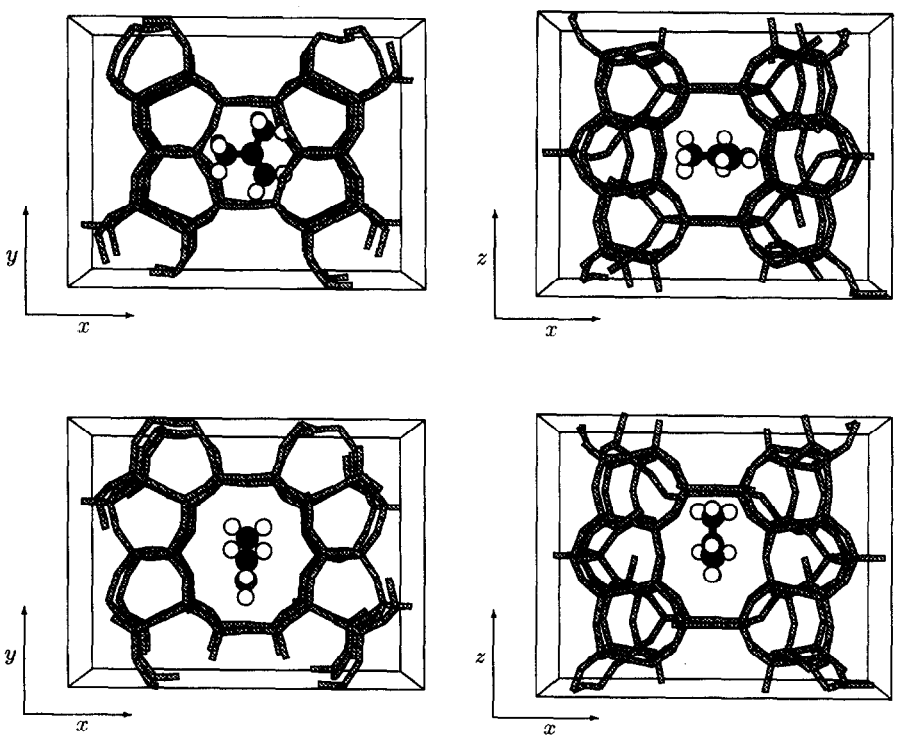

Fig. 1. Minimum energy sites of isobutene in FER, as determined by an energy minimization with the cff91-czeo Biosym forcefield. The presented structure covers two unit-cells of FER along [001]. For clarity, the bottom views are translated of 0.5 unit-cells along [010] with respect to the top views. Top: minimum energy site in the cavities along the 8-T channels ($E = -49.3$ kJ/mol); left: view along [001]; right: view along [010]. Bottom: minimum energy site at the intersection between the 10- and 8-T channels ($E = -44.6$ kJ/mol); left: view along [001]; right: view along [010].

twelfth power of the C–Hz and H–Hz distances, which characterizes the repulsive interaction in the channels, is $\Sigma_i d_i^{-12}$(C–Hz) = 1.28 $\times 10^{-6}$ Å^{-12} in the site along the 10-T channel versus 1.56 $\times 10^{-6}$ Å^{-12} in the cavity along the 8-T channel, and $\Sigma_i d_i^{-12}$(H–Hz) = 1.83 $\times 10^{-6}$ Å^{-12} versus 2.55 $\times 10^{-6}$ Å^{-12} in the same sites.

Note that the MES in MEL and in the straight channels of MFI are very similar, being in both cases between two 5-T rings, and that the corresponding energies are also similar (−39.8 versus −39.3 kJ/mol). In the case of MFI and MEL, the MES are located in the channels out of the intersections.

The shape complementarity is best illustrated by the comparison between the different butene isomers. In all cases except TON, 1-butene has the largest interaction energy; this can be explained by its ability to deform itself, which increases its affinity to the pore wall. In all cases except MTT and FER, isobutene has the smallest interaction energy, which is once again explained by its low affinity to the pore wall, as all its atoms are unable to get close to the wall at the same time.

5. Self-diffusion

In Table 3 the self-diffusion coefficients calculated from the molecular dynamics simulation at 623 K are reported. As indicated previously, two methods were used to determine the diffusivities from the MD runs: by least-square linear regression of the MSD of the center of mass

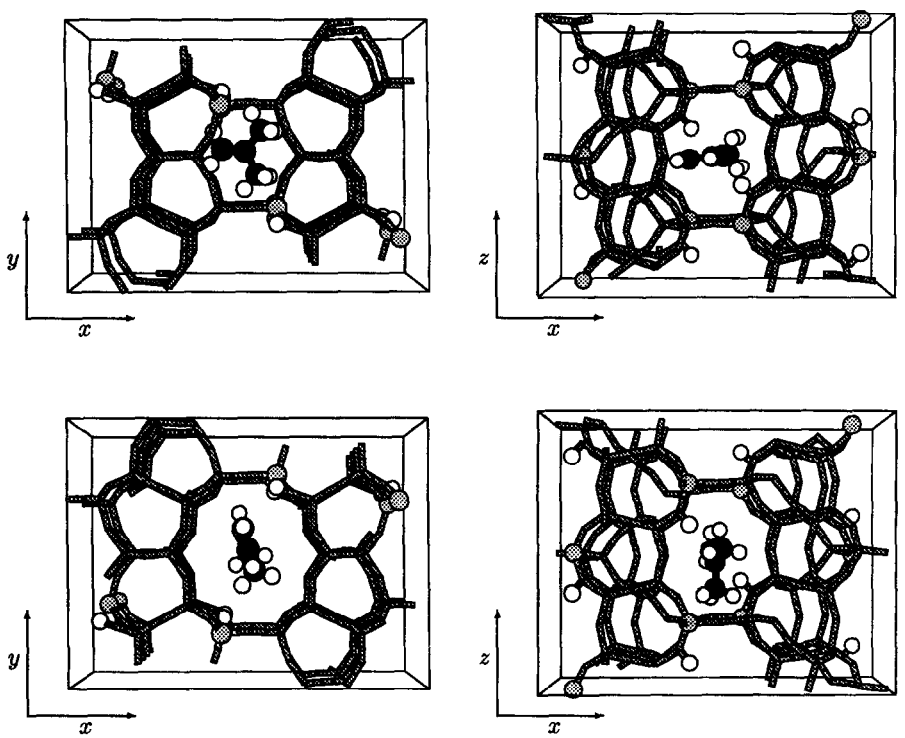

Fig. 2. Minimum energy sites of isobutene in H-FER, as determined by an energy minimization with the cff91-czeo Biosym forcefield. The presented structure covers two unit-cells of H-FER along [001]. For clarity, the bottom views are translated of 0.5 unit-cells along [010] with respect to the top views. The shaded spheres in the structure mark the position of the Al atoms, the white spheres those of the hydrogens. Top: minimum energy site in the cavities along the 8-T channels (E = −27.4 kJ/mol); left: view along [001]; right: view along [010]. Bottom: minimum energy site at the intersection between the 10- and 8-T channels (E = −33.7 kJ/mol); left: view along [001]; right: view along [010].

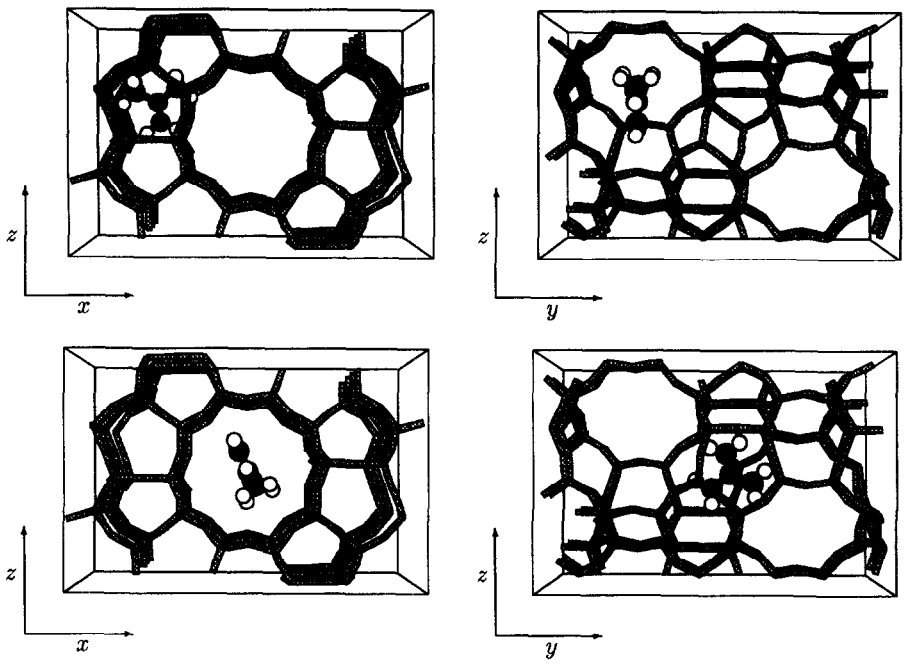

Fig. 3. Minimum energy sites for isobutene in MFI, as determined by an energy minimization with the cff91-czeo Biosym forcefield. Top: minimum energy site in the [100] zigzag channel ($E = -41.0$ kJ/mol); left: view along [010]; right: view along [100]. Bottom: minimum energy site in the [010] straight channel ($E = -39.3$ kJ/mol); left: view along [010]; right: view along [100].

(COM) of each butene isomer versus time, between 50 and 150 ps, and by integration of the VACF of the COM. These two methods, applied on the very same simulation results, give values that are quite different from each other; however, the two values are of the same order of magnitude, and in most of the cases conserve the ranking between the different isomers. In certain cases, we did not observe any diffusion during the time of the MD runs; the corresponding diffusion coefficients are denoted by 'und.' in Table 3. An upper limit of the corresponding diffusivities may be estimated by remarking that these molecules stayed in the same unit-cell during the 200 ps run. These two observations emphasize that the computed self-diffusion coefficient is more qualitative than really quantitative. Nevertheless, we believe that it can be

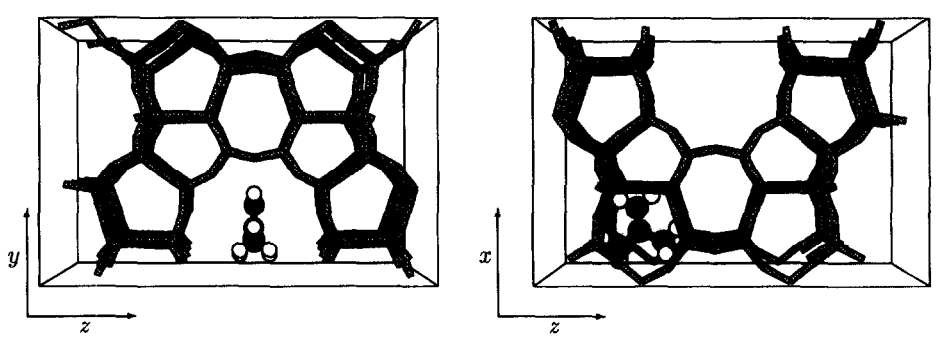

Fig. 4. Minimum energy site for isobutene in MEL, as determined by an energy minimization with the cff91-czeo Biosym forcefield ($E = -39.8$ kJ/mol). Left: view along [100]; right: view along [010].

used for purpose of comparison between the different isomers in the same zeolite, and between different zeolites for the same isomer.

The diffusion coefficients of butene in MFI can be compared to the experimental data obtained by pulse chromatography by Hufton et al. [38]. These authors have studied diffusion of 2-butene and isobutene in silicalite between 450 and 500 K. Extrapolation of their results to 623 K gives a value of approximately 0.2×10^{-8} m^2/s for the upper limit of the diffusivity of *cis*- and *trans*-2-butene, and a diffusivity of approximately 0.03×10^{-8} m^2/s for isobutene. These values are in quite good agreement with the computed ones. Note that the interaction energies presented in Table 2 are underestimated by approximately 30% by comparison to the heat of adsorption determined experimentally by Hufton et al. ($\approx$ 70 kJ/mol).

In all zeolites considered here except TON, *trans*-2-butene diffuses faster than all other isomers. This is probably due to its linear undeformable shape, which facilitates its diffusion through the channels. Although 1-butene is also linear, its deformation, which is the cause for its higher interaction energy with the zeolite wall, hinders partly its diffusion. In all cases, isobutene diffuses more slowly than the other isomers, which is simply due to its larger kinetic diameter; only in zeolites TON and MTT could we compute an approximate value of its diffusion coefficient. We note that for all molecules, the diffusion is considerably slower in H-FER than in FER, while the dimensions of the 10-T channel is similar (cf. Table 2); hence, this can be unambiguously attributed to the influence of the protons in the channel. In both FER and H-FER, the molecules could not cross the 8-T rings during the 200 ps of the MD run, due to the high energy barrier to the crossing of this ring [16].

There does not seem to be any direct link between the diffusivities and the channel size nor the minimum interaction energies, as long as the channels are large enough to let the molecules through. This may be related to the anomalous diffusion behavior of molecules in confined geometry first asserted by Derouane and co-workers [39], and recently observed by molecular dynamics simulations in A-type zeolites by Yashonath and coworkers [40]. However this may also come from the shape of the sorbed molecules, and their corresponding affinity to the zeolite walls, which we have seen explains their interaction energies. In favor of this explanation are the quite anomalous diffusivities computed in TON: in this zeolite, and in contradiction with the others, *cis*-2-butene diffuses faster than *trans*-2-butene, and we observed a certain diffusion of isobutene. Thus the channel of TON seems to favor the diffusion of somewhat bulkier molecules, as compared to

Table 3
Self-diffusion coefficients ($Å^2/ps$ or 10^{-8} m^2/s) of the butene isomers in the zeolite channels, computed from a 200 ps molecular dynamics run at 623 K. MSD indicates the diffusion coefficient determined from a linear fit of the MSD versus time between 50 and 150 ps, VACF, the diffusion coefficient calculated by integration of the VACF. 'und.' means that we did not observe any diffusion during the MD run

Zeolite code	1-butene		*Cis*-2-butene		*Trans*-2-butene		Isobutene	
	MSD	VACF	MSD	VACF	MSD	VACF	MSD	VACF
TON	0.17	0.17	1.09	0.80	0.17	0.08	0.14	0.11
MTT	0.29	0.24	0.62	0.35	1.87	1.36	0.10	0.04
MEL	0.36	0.84	0.10	0.12	2.45	1.42	und.	und.
MFI	0.97	0.77	0.44	0.58	1.33	1.80	und.	und.
FER	0.95	0.88	0.58	1.09	1.77	2.21	und.	und.
H-FER	0.07	0.08	0.05	0.09	0.67	0.93	und.	und.
HEU	und.	und.	und.	und.	0.26	0.29	und.	und.

the other structures studied here. Consequently, the diffusion of isobutene is most favorable in TON, in regard of all other zeolite structures.

The density of vibrational states (DOS) of the center of mass of the butene isomers was computed by a Fourier transform of the velocity autocorrelation function, and convoluted with a 30 cm^{-1} gaussian function in order to retain only the broadest and therefore most meaningful features of the spectra. Figs. 5–8 display the low-frequency DOS ($\sigma < 200$ cm^{-1}) for each butene isomer in the zeolites H-FER, FER, MEL, MTT, TON, and MFI. At these low frequencies, the spectra show the external vibrations of the COM of the sorbed molecules within the zeolite channels. Due to the existence of privileged directions in the structure, they are very different along the different axes. In the directions perpendicular to the channel axes, peaks between 50 and 110 cm^{-1} characterize

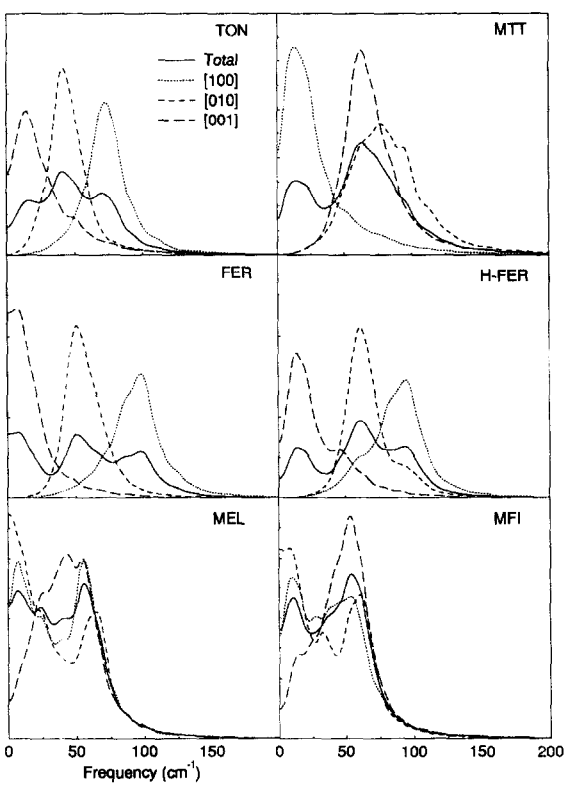

Fig. 5. Vibrational density of states of the center of mass of 1-butene in channel zeolites, as computed from a 200 ps MD run at 623 K, with the forcefield cff91-czeo of Biosym.

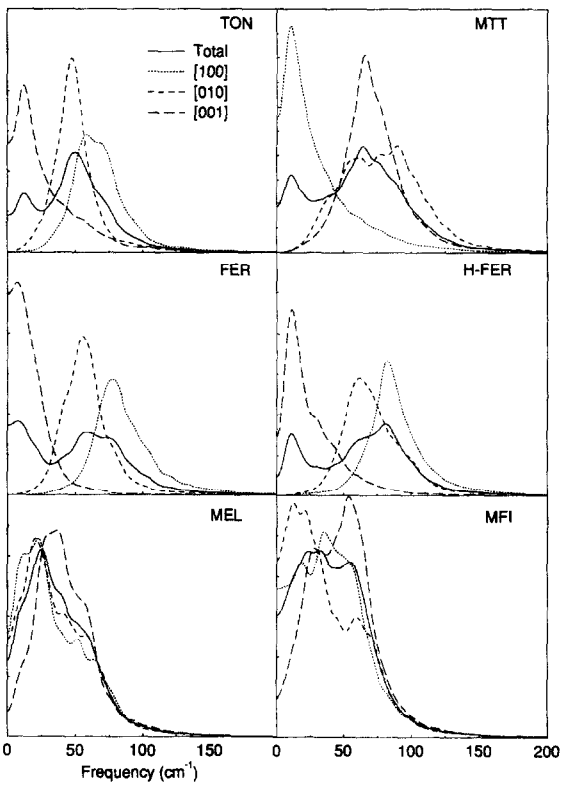

Fig. 6. Vibrational density of states of the center of mass of *cis*-2-butene in channel zeolites, as computed from a 200 ps MD run at 623 K, with the forcefield cff91-czeo of Biosym.

the vibrating motions between the channel walls. Their frequency depends mainly on the size of the guest molecules and the size of the pore, and hence, it can be observed on the unidirectional channel zeolites TON and MTT that the vibrations of *trans*-2-butene and 1-butene perpendicular to the channel axis (which is [001] and [100], respectively) have significantly lower frequencies than those of *cis*-2-butene and isobutene.

In the two unidirectional channel zeolites TON and MTT, the spectra along the channel axis are made of a diffusive component, but also show a vibration peak at low frequencies ($\sigma < 20$ cm^{-1}) indicating a vibrative motion along this axis. At the temperature of 623 K, a 20 cm^{-1} frequency corresponds to a vibration of about 5 Å of the COM of the butene molecules, which is approximately the size of the unit-cell along the channel axis. This is

important, as it shows that, even at 623 K, the channels can be represented as a row of separated sites in which the molecules reside and vibrate before jumping to a neighboring site.

Although ferrierite is a two-channel type zeolite, we only observed diffusion along its 10-T channels. The low frequency spectra of sorbed butenes in FER is then made of three well-defined peaks due to vibrations along the three spatial directions, plus a diffusive very low frequency component along the channel axis [001]. There is much similarity between the vibration peaks in FER and H-FER, further showing that, with the forcefield used here, the protons do not attract the sorbed molecules.

As zeolite MEL presents two identical channels along [100] and [010], the corresponding components on the spectra are identical; they are made of a vibration peak, probably corresponding to the rattling motions perpendicular

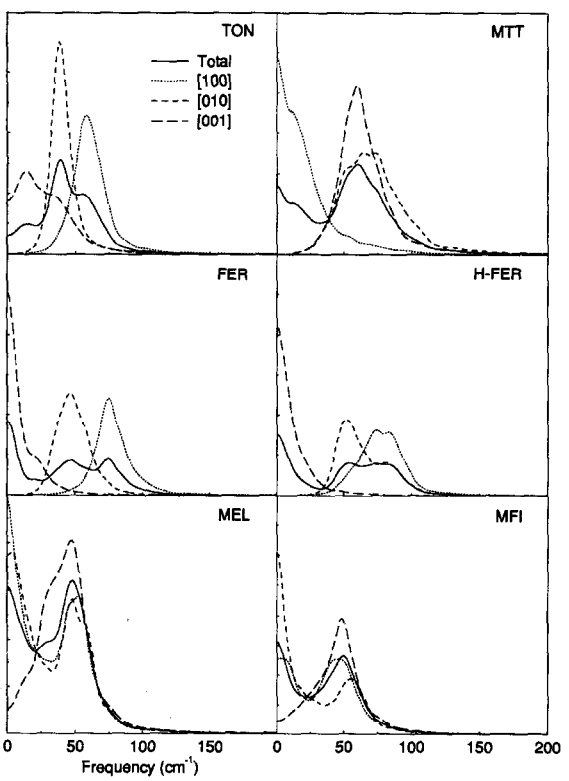

Fig. 7. Vibrational density of states of the center of mass of *trans*-2-butene in channel zeolites, as computed from a 200 ps MD run at 623 K, with the forcefield cff91-czeo of Biosym.

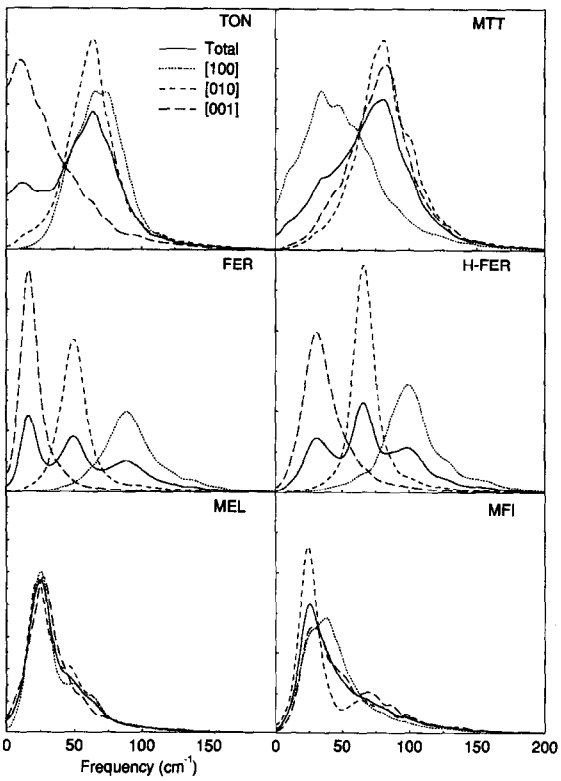

Fig. 8. Vibrational density of states of the center of mass of isobutene in channel zeolites, as computed from a 200 ps MD run at 623 K, with the forcefield cff91-czeo of Biosym.

to the channel axis, and of a diffusive component corresponding to the motion along the channel axis. There is no apparent peak that can be attributed to a vibration along the channel axis. This may indicate that in this larger pore zeolite, the diffusion does not proceed by jumps between separated sites; however, it is most probably hidden by the vibration peak perpendicular to the channel axis. The same features can be observed on the DOS in MFI, but the different nature of the channels of this zeolite and the existence of a zigzag type channel hide most of the informations.

6. Conclusion

We have calculated the minimum interaction energies and the diffusivities of butene isomers in TON, MTT, MEL, MFI, FER, H-FER, and

HEU, by molecular mechanics and dynamics, using the cff91-czeo forcefield of Biosym Technologies. This forcefield has been shown to well reproduce the cell parameters of these zeolite structures, but lead to interaction energies lower than the experimental ones. Furthermore, the electrostatic part of the interaction energy between guest butene molecules and the zeolite protons is most probably not accurately taken into account.

Considering that the guest molecule–host structure energy arises mainly from steric requirements, the interaction energies and the minimum energy positions are readily explained by confinement effects and by the affinity between the 'shape' of the guest molecule with the zeolite wall. This explains in simple terms why in all except the smallest cavities isobutene is less sorbed than the other isomers.

Although the 200 ps molecular dynamics runs can only probe the short-time diffusion of the butene isomers in the zeolite channels, significative results can be derived from this study. In all structures except TON, *trans*-2-butene diffuses faster than all other isomers, probably because of its linear indeformable shape. No link is found between the interaction energy or the channel dimensions and the diffusivities. In all cases except for zeolites TON and MTT, we could not probe isobutene diffusion during the 200 ps dynamics runs. In zeolite TON, the ratio of isobutene versus linear butene diffusion is the largest, and hence diffusion probably does not constitute the rate-limiting process for skeletal isomerization of butene in this zeolite.

We have shown previously [16] that the diffusion of butene in ferrierite is influenced by diffusion processes taking place on a longer time-scale than can be probed by a 200 ps MD run, due to the presence of stable adsorption sites separated by high diffusion barriers from the main 10-T channels. Similar processes probably influence the diffusion in the other type of zeolites. Even when no second stable site exists, like in the unidirectional channel zeolites TON or MTT, the influence of the number of molecules per channel has to be investigated, as the single-file diffusion may change the results obtained here for a fixed coverage. The low-frequency density of states of the sorbed butene isomers shows that the diffusive motion can be regarded, in a first approximation, as jumps between sites in which the molecules reside; this justifies the use of a jump diffusion model to investigate the numerous parameters that influence the long-time diffusion.

Acknowledgements

All authors wish to thank the FUNDP for the use of the Namur Scientific Computing Facility Center (SCF). They acknowledge financial support of the FNRS-FRFC, the "Loterie Nationale" for the convention No. 9.4593.92, the FNRS within the framework of the "Action d'impulsion à la recherche fondamentale" of the Belgian Ministry of Science under the convention No. D.4511.93, IBM Belgium for the Academic Joint Study on "Cooperative Processing for Theoretical Physics and Chemistry", and Biosym Technologies Inc., for the use of their software in the framework of the "Catalysis and Sorption" consortium. F.J. acknowledges Professor A. Lucas, Director of the PAI 3–49, and the European Union for the attribution of a post-doctoral fellowship in the framework of the HCM/Host Institution ERB CHBG CT930343 "Science of Interfacial and Mesoscopic Structures".

References

[1] J. Haggin, C&E News 71 (1993) 28.
[2] S. Natarajan, P.A. Wright and J.M. Thomas, J. Chem. Soc. Chem. Commun. (1993) 1861.
[3] W.-Q. Xu, Y.-G. Yin, S.L. Suib and C.-L. O'Young, J. Catal. 150 (1994) 34.
[4] D. Bianchi, M.W. Simon, S.S. Nam, W.-Q. Xu, S.L. Suib and C.-L. O'Young, J. Catal. 145 (1994) 551.
[5] M.W. Simon, S.L. Suib and C.-L. O'Young, J. Catal. 147 (1994) 484.

[6] C.-L. O'Young, W.-Q. Xu, M.W. Simon and S.L. Suib, Stud. Surf. Sci. Catal. 84 (1994) 1671.
[7] S.M. Yang, D.H. Guo, J.S. Lin and G.T. Wang, Stud. Surf. Sci. Catal. 84 (1994) 1677.
[8] H.H. Mooiweer, K.P. de Jong, B. Kraushaar-Czarnetzki, W.H.J. Stork and B.C.H. Krutzen, Stud. Surf. Sci. Catal. 84 (1994) 2327.
[9] W.-Q. Xu, Y.-G. Yin, S.L. Suib and C.-L. O'Young, J. Phys. Chem. 99 (1994) 758.
[10] W.-Q. Xu, Y.-G. Yin, S.L. Suib, J.C. Edwards and C.-L. O'Young, J. Phys. Chem. 99 (1994) 9443.
[11] C.-L. O'Young, R.J. Pellet, D.G. Casey, J.R. Ugolini and R.A. Sawicki, J. Catal. 151 (1995) 467.
[12] R.J. Pellet, D.G. Casey, H.-M. Huang, R.V. Kessler, E.J. Kuhlman, C.-L. O'Young, R.A. Sawicki and J.R. Ugolini, J. Catal. 157 (1995) 423.
[13] M. Guisnet, P. Andy, N.S. Gnep, C. Travers and E. Benazzi, J. Chem. Soc. Chem. Commun. (1995) 1685.
[14] H.C. Woo, K.H. Lee and J.S. Lee, Appl. Catal. A 134 (1996) 147.
[15] W.M. Meier and D.H. Olson, Atlas of Zeolite Structure Types, 3rd Ed., Butterworth-Heinemann, London, 1992.
[16] F. Jousse, L. Leherte and D.P. Vercauteren, Mol. Simul., 17 (1996) 175.
[17] Discover user guide, version 95.0, Biosym/MSI, San Diego (1995).
[18] J.-R. Hill and J. Sauer, J. Phys. Chem. 98 (1994) 1238; 99 (1995) 9536.
[19] C.M. Freeman, C.R.A. Catlow, J.M. Thomas and S. Brode, Chem. Phys. Lett. 186 (1991) 137.
[20] M.P. Allen and D.J. Tildesley, Computer Simulations of Liquids, Clarendon Press, Oxford, 1987.
[21] B. Marler, Zeolites 7 (1987) 393.
[22] R.M. Highcock, G.W. Smith and D. Wood, Acta Cryst. C 41 (1985) 1391.
[23] A.C.J. Rohrman, R.B. LaPierre, J.L. Schlenker, J.D. Wood, E.W. Valyocsik, M.K. Rubin, J.B. Higgins and W.J. Rohrbaugh, Zeolites 5 (1985) 352.
[24] C.A. Fyfe, H. Gies, G.T. Kokotailo, C. Pasztor, H. Strobl and C.E. Cox, J. Am. Chem. Soc. 111 (1989) 2470.
[25] O. Terasaki, T. Ohsuna, H. Sakuma, D. Watanabe, Y. Nakagawa and R.C. Medrud, Chem. Mater. 8 (1996) 463.
[26] H. van Koningsveld, H. van Bekkum and J.C. Jansen, Acta Cryst. B 43 (1987) 127.
[27] D.H. Olson, G.T. Kokotailo, S.L. Lawton and W.M. Meier, J. Phys. Chem. 85 (1981) 2238.
[28] R.E. Morris, S.J. Weigel, N.J. Henson, L.M. Bull, M.T. Janicke, B.F. Chmelka and A.K. Cheetham, J. Am. Chem. Soc. 116 (1994) 11849.
[29] A. Kuperman, S. Nadimi, S. Oliver, G.A. Ozin, J.M. Garcés and M.M. Olken, Nature 365 (1993) 239.
[30] P.A. Vaughan, Acta Cryst. 21 (1966) 983.
[31] A. Alberti and C. Sabelli, Z. Krist. 178 (1987) 249.
[32] R. Gramlich-Meier, W.M. Meier and B.K. Smith, Z. Krist. 169 (1984) 201.
[33] T.W. Hambley and J.C. Taylor, J. Solid State Chem. 54 (1984) 1.
[34] L. Abrams and D.R. Corbin, J. Inc. Phenom. Mol. Recogn. Chem. 21 (1995) 1.
[35] R.A. van Santen, in: J.C. Jansen, M. Stöcker, H.G. Karge and J. Weitkamp (Eds.), Stud. Surf. Sci. Catal. 85 (1994) 273; J. Sauer, P. Ugliengo, E. Garrone and V.R. Saunders, Chem. Rev. 90 (1994) 2827; E. Brunner, J. Mol. Struct. 355 (1995) 61; M. Hunger and T. Horvath, Ber. Bunsenges. Phys. Chem. 99 (1995) 1316.
[36] F. Jousse and E. Cohen de Lara, J. Phys. Chem. 100 (1996) 233; F. Jousse, A.V. Larin and E. Cohen de Lara, J. Phys. Chem. 100 (1996) 238.
[37] P. Ugliengo, A.M. Ferrari, A. Zecchina and E. Garrone, J. Phys. Chem. 100 (1996) 3632.
[38] J.R. Hufton, D.M. Ruthven and R.P. Danner, Microporous Mater. 5 (1995) 39.
[39] E.G. Derouane, J.-M. André and A.A. Lucas, J. Catal. 110 (1988) 58; I. Derycke, J.-P. Vigneron, Ph. Lambin, A.A. Lucas and E.G. Derouane, J. Chem. Phys. 94 (1991) 4620.
[40] P. Santikary and S. Yashonath, J. Phys. Chem. 98 (1994) 9252; S. Yashonath and S. Bandyopadhyay, Chem. Phys. Lett. 228 (1994) 284.